The Journal of Immunology

RESEARCH ARTICLE | AUGUST 15 2017

The Effect of Inhibitory Signals on the Priming of Drug Hapten–Specific T Cells That Express Distinct Vβ Receptors FREE

Andrew Gibson; ... et. al

J Immunol (2017) 199 (4): 1223–1237.
https://doi.org/10.4049/jimmunol.1602029

The Effect of Inhibitory Signals on the Priming of Drug Hapten–Specific T Cells That Express Distinct Vβ Receptors

Andrew Gibson,* Lee Faulkner,* Maike Lichtenfels,* Monday Ogese,*,† Zaid Al-Attar,* Ana Alfirevic,* Philipp R. Esser,‡ Stefan F. Martin,‡ Munir Pirmohamed,* B. Kevin Park,* and Dean J. Naisbitt*

Drug hypersensitivity involves the activation of T cells in an HLA allele–restricted manner. Because the majority of individuals who carry HLA risk alleles do not develop hypersensitivity, other parameters must control development of the drug-specific T cell response. Thus, we have used a T cell–priming assay and nitroso sulfamethoxazole (SMX-NO) as a model Ag to investigate the activation of specific TCR Vβ subtypes, the impact of programmed death -1 (PD-1), CTL-associated protein 4 (CTLA4), and T cell Ig and mucin domain protein-3 (TIM-3) coinhibitory signaling on activation of naive and memory T cells, and the ability of regulatory T cells (Tregs) to prevent responses. An expansion of the TCR repertoire was observed for nine Vβ subtypes, whereas spectratyping revealed that SMX-NO–specific T cell responses are controlled by public TCRs present in all individuals alongside private TCR repertoires specific to each individual. We proceeded to evaluate the extent to which the activation of these TCR Vβ–restricted Ag-specific T cell responses is governed by regulatory signals. Blockade of PD-L1/CTLA4 signaling dampened activation of SMX-NO–specific naive and memory T cells, whereas blockade of TIM-3 produced no effect. Programmed death-1, CTLA4, and TIM-3 displayed discrete expression profiles during drug-induced T cell activation, and expression of each receptor was enhanced on dividing T cells. Because these receptors are also expressed on Tregs, Treg-mediated suppression of SMX-NO–induced T cell activation was investigated. Tregs significantly dampened the priming of T cells. In conclusion, our findings demonstrate that distinct TCR Vβ subtypes, dysregulation of coinhibitory signaling pathways, and dysfunctional Tregs may influence predisposition to hypersensitivity. ***The Journal of Immunology*****, 2017, 199: 1223–1237.**

Drug hapten–specific T cell responses are detectable in patients who present with hypersensitivity reactions affecting skin and internal organs. It is important to emphasize that reactions do not develop in all patients; they are idiosyncratic in nature, with a prevalence of 1 in 10,000–100,000 individuals (1). Recent studies focusing on mechanisms of β-lactam hypersensitivity have shown that a threshold level of antigenic drug–protein adduct is exceeded in all patients exposed to a therapeutic drug course (2), and all individuals have T cells within their repertoire that can be activated with drugs (3). Thus, it is now important to investigate the immunological parameters that determine whether the formation of protein adducts in vivo will result in a drug-specific T cell response and tissue injury.

In recent years, progress in this field has centered on the association of multiple drugs with specific HLA alleles. However, with the exception of HLA-B*57:01–restricted abacavir and HLA-B*15:02–restricted carbamazepine (CBZ) hypersensitivity (4–6), the majority of individuals who carry known HLA risk alleles do not develop hypersensitivity when exposed to a culprit drug. Indeed, T cell stimulation can be influenced by a multitude of factors that can be divided into signals 1 and 2. Signal 1 refers to the interaction of a TCR with a corresponding peptide–HLA complex. Whether the expression of specific TCRs influences susceptibility to drug hypersensitivity remains largely unexplored. A recent study reported that CBZ hypersensitivity only occurs in individuals who express both a particular HLA variant and a specific TCR Vβ (7). However, this is not the case for abacavir hypersensitivity (8). Although signal 1 is required for T cell signaling, signal 2 determines whether this ultimately translates into T cell activation; thus, it is the nature of both signals that ultimately determines the unique T cell activation threshold for an individual. Signal 2 is composed of costimulatory and coinhibitory pathways that signal simultaneously to regulate T cell activation in a complex balancing act between tolerance and activation. We have shown that blockade of the programmed death-1 (PD-1) pathway via PD-L1, but not PD-L2, enhances the priming of naive T cells to drug Ags. Although PD-1 is an important immune checkpoint, complex interplay between pathways means that it is crucial to elucidate the role of additional cosignaling pathways, as well as how they interact, to effectively analyze the role of regulatory signaling

*Department of Molecular and Clinical Pharmacology, Medical Research Council Centre for Drug Safety Science, University of Liverpool, Liverpool L69 3GE, United Kingdom; †Pathology Sciences, Drug Safety and Metabolism, AstraZeneca Research and Development, Cambridge CB4 0WG, United Kingdom; and ‡Allergy Research Group, Department of Dermatology, Medical Center–University of Freiburg, Freiburg im Breisgau, 79104 Freiburg, Germany

ORCIDs: 0000-0002-0111-5382 (Z.A.-A.); 0000-0002-2801-9817 (A.A.); 0000-0002-1617-1280 (S.F.M.); 0000-0002-7534-7266 (M.P.).

Received for publication November 30, 2016. Accepted for publication June 11, 2017.

This work was supported by the Medical Research Council Centre for Drug Safety Science (Grant G0700654) and by the Mechanism-Based Integrated Systems for the Prediction of Drug Induced Liver Injury project (supported by the European Community under the Innovative Medicines Initiative Programme through Grant Agreement 115336).

Address correspondence and reprint requests to Dr. Dean J. Naisbitt, Department of Molecular and Clinical Pharmacology, Medical Research Council Centre for Drug Safety Science, Sherrington Building, Ashton Street, University of Liverpool, Liverpool L69 3GE, U.K. E-mail address: dnes@liv.ac.uk

The online version of this article contains supplemental material.

Abbreviations used in this article: CBZ, carbamazepine; CTLA4, CTL-associated protein 4; DC, dendritic cell; MFI, mean fluorescence intensity; PD-1, programmed death-1; SMX, sulfamethoxazole; SMX-NO, nitroso sulfamethoxazole; TEN, toxic epidermal necrolysis; TIM-3, T cell Ig and mucin domain protein-3; Treg, regulatory T cell.

during T cell activation. Additionally, because it has recently been reported that certain reactions may be caused by a drug Ag stimulating pre-existing memory T cells (9), it is critical to assess the role of regulatory pathways during primary and secondary T cell responses.

Similar to the PD-1–PD-L1 interaction, CTL-associated protein 4 (CTLA4) represents a critical checkpoint in T cell regulation, because the individual knockdown of these receptors leads to overwhelming lymphoproliferation in mice, ultimately resulting in death (10–12). CTLA4 has two ligands, CD80 and CD86, which it shares with the costimulatory receptor CD28; thus, these opposing pathways act to competitively inhibit one another (13). Although there is a wide range of other coinhibitory pathways, the role of the lesser-known receptor, T cell Ig and mucin domain protein-3 (TIM-3), which mediates its function through binding to galectin-9 leading to the death of predominantly Th1-specific T cells, is particularly interesting. This is because activation of TIM-3 has been reported to act synergistically alongside PD-1 on tumor-infiltrating lymphocytes, inferring that, together, these pathways represent a formidable immunological barrier to T cell activation (14).

In addition to direct signaling between dendritic cells (DCs) and effector T cells, coinhibitory pathways are used by $CD25^+$ regulatory T cells (Tregs). This subset of Th cells functions to suppress effector T cell responses and is physiologically important for the establishment of feto–maternal tolerance and dampening T cell responses after Ag clearance (15). Recent research suggests that dysfunctional Tregs may have a role in specific drug hypersensitivity reactions, with Takahashi's group reporting that Tregs are functionally defective at the cutaneous sites of toxic epidermal necrolysis (TEN) (16). Furthermore, models of TEN found that Tregs can prevent TEN-associated epidermal injury (16, 17); therefore, susceptibility in patients may be linked to a defect in Tregs, potentially through abnormal coinhibitory signaling. Indeed, polymorphisms in coinhibitory pathways are associated with the dysregulation of T cell activation and the onset of T cell–induced autoimmune diseases (18–21). However, how these receptors affect drug Ag–specific T cell activation remains unknown.

Because single genetic associations cannot fully account for the majority of drug-induced hypersensitivities, it is becoming increasingly apparent that the etiologies of such reactions are likely multifaceted, meaning that the presence of a sole risk factor alone will not predispose an individual to develop hypersensitivity. Therefore, it is critical to examine how different elements of signal 1 and signal 2 interact during T cell priming to a specific drug and to characterize the phenotype of the T cells responsible for eliciting drug hypersensitivity reactions. Using the chemically defined model drug Ag nitroso sulfamethoxazole (SMX-NO) and an in vitro priming assay that uses T cells and autologous DCs from healthy individuals (22), we have investigated the effects of the above-mentioned parameters on drug Ag–induced T cell activation. Specifically, we probed for the preferential use of specific TCR Vβ subtypes, expanded on our previous PD-1 study by comparing the role of PD-1–PD-L1 signaling during the activation of naive and memory T cells from healthy donors, investigated CTLA4 and TIM-3 coinhibitory signaling, and quantified the suppressive capacity of $CD25^+$ Tregs.

Materials and Methods

Human subjects

One hundred twenty milliliters of venous blood was donated by SMX-naive human donors, all of whom had given informed written consent to partake in this study approved by the Liverpool local research ethics committee. A previous lack of sensitization in donors who later produced SMX-responsive T cells was confirmed by a negative lymphocyte transformation test in response to SMX (1–1.5 mM) and SMX-NO (20–40 μM). This was observed despite a significant response following exposure to tetanus toxoid (positive control).

Cell separation

PBMCs were separated from whole blood using Lymphoprep (Axis Shield, Dundee, U.K.) and density gradient separation. Distinct cell populations were isolated using magnetic bead separation columns performed in line with the manufacturer's instructions (Miltenyi Biotec, Bisley, U.K.). Briefly, total PBMCs were subjected to positive selection for $CD14^+$ monocytes, after which the non-$CD14^+$ population was incubated with an anti-T cell Ab mixture to negatively select for $CD3^+$ pan T cells. Lastly, pan T cells were subject to two further consecutive positive-selection steps: $CD25^+$ selection for isolation of Tregs and $CD45RO^+$ selection on the $CD25^-$ population for isolation of memory T cells ($CD45RO^+$) from the remaining naive ($CD45RO^-$) T cell population. A total of 2×10^6 naive T cells from donors selected for TCR Vβ spectratyping analysis was frozen in RNAlater (stored at −80°C), whereas all other cells were frozen in 10% DMSO and stored at −150°C before use.

In vitro T cell–priming assay

To generate DCs, $CD14^+$ monocytes were cultured ($3–5 \times 10^6$ per well; six-well plate; total volume, 6 ml; 37°C/5% CO_2) for 8 d in R9 medium (RPMI 1640, 100 μg/ml penicillin, 100 U/ml streptomycin, 25 μg/ml transferrin, 10% human AB serum [Innovative Research], 25 mM HEPES buffer, 2 mM L-glutamine) supplemented with GM-CSF and IL-4 (800 U/ml) (PeproTech). To induce DC maturation, 25 ng/ml TNF-α (PeproTech) and 1 μg/ml LPS (*Escherichia coli* 0111:B4; Sigma-Aldrich) were added on the penultimate day of culture. Naive or memory $CD3^+$ T cells, with Tregs removed, were cultured (2.5×10^6 per well; 24-well plate; total volume, 2 ml) with autologous mature DCs (0.8×10^5 per well) and SMX-NO (50 μM) for 8 d. Human targeted anti–PD-L1 (5 μg/ml), anti-CTLA4 (10 μg/ml), or anti–TIM-3 Ab (7.5 μg/ml) (all from BioLegend, London, U.K.) were added to specific wells prior to the addition of SMX-NO and incubated for ≥30 min (37°C/5% CO_2). To identify the optimal Ab concentration for blocking, dose-ranging studies were performed using various Ab concentrations, including the concentration indicated for use by the supplier. Alternatively, specific quantities of autologous $CD25^+$ Tregs were added to individual wells. Experiments were repeated a minimum of three times.

T cell readouts

SMX-NO–primed naive or memory T cells were harvested and plated (1×10^6 per well; 96-well plate; total volume, 200 μl) with autologous mature DCs (4×10^3 per well) and SMX-NO (20–50 μM) for assessment of proliferative capacity by [^{3}H]thymidine incorporation (triplicate cultures) or CFSE incorporation or by analysis of cytokine/cytolytic molecule secretion using ELISPOT (duplicate cultures) after incubations of 48, 72, and 96 h, respectively (37°C/5% CO_2). PHA (20 μg/ml) was used as a positive control. The secretion of IFN-γ, IL-13, and granzyme B was visualized by following the ELISPOT procedure provided by the manufacturer (Mabtech, Nacka Strand, Sweden). [^{3}H] Thymidine (0.5 μCi per well) was added to the proliferation plate, which was subjected to a 16-h incubation before analysis of incorporated radioactivity using a MicroBeta TriLux 1450 LSC beta counter (PerkinElmer, Cambridge, U.K.). CFSE analysis was conducted on a FACSCanto II flow cytometer (BD Biosciences, Oxford, U.K.) using a previously established protocol (22). T cell phenotype was assessed at various time points through the priming process by staining with anti-CD3–allophycocyanin, CD4-VioBlue, CD8-PerCPCy5, PD-1–PE, CTLA4-allophycocyanin, and TIM-3–PE Abs.

For TCR Vβ spectratyping analysis, SMX-NO–primed naive T cells were restimulated with fresh mature DCs (DC/T cell ratio 1:25) and SMX-NO (50 μM; 24-well plate) for 72 h before being subjected to

Table I. Coverage of the TCR Vβ repertoire in T cells before (naive) and after (memory) priming to SMX-NO

	TCR Vβ coverage (%)					
	S1	S2	S3	S4	S5	S6
Naive	61	56	52	57	53	50
Memory	65	83	78	71	76	65

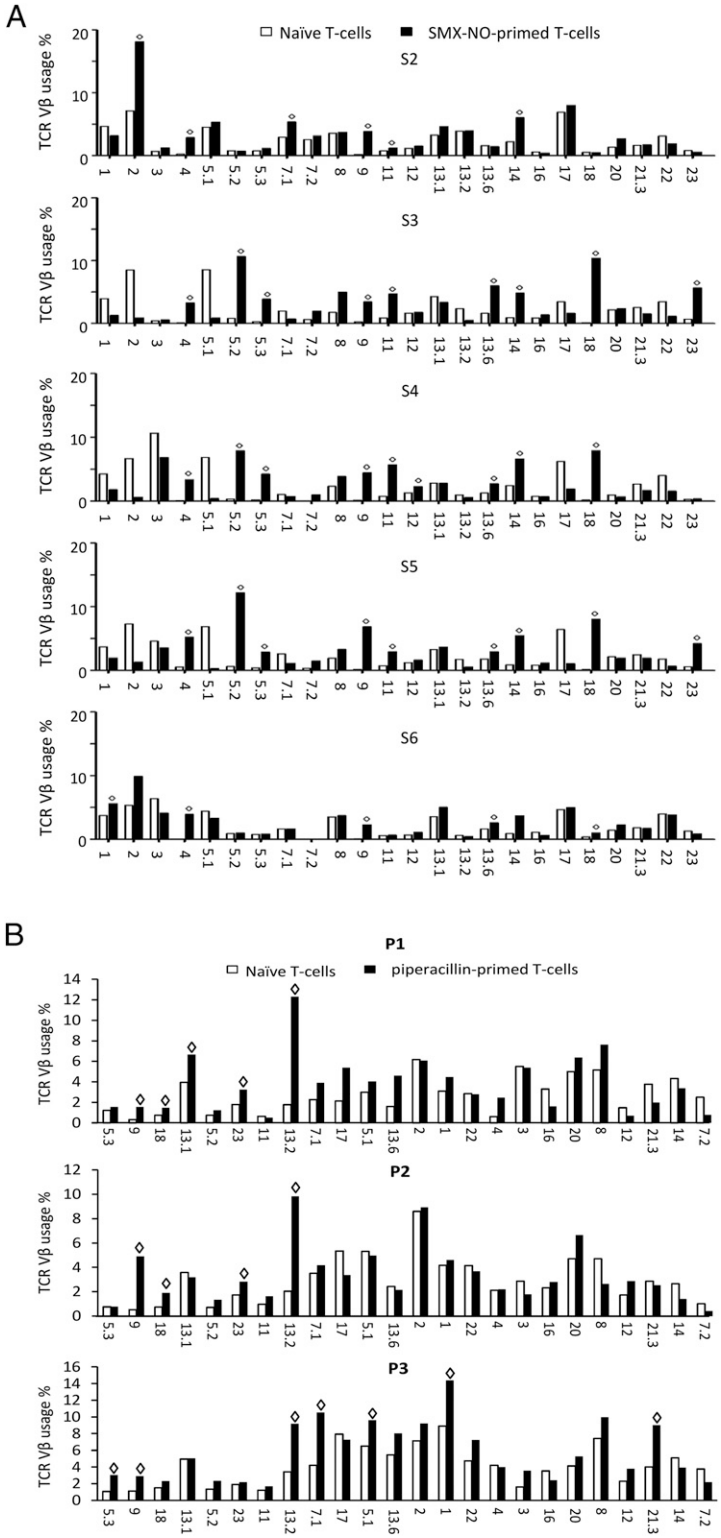

FIGURE 1. Clonogram of naive and SMX-NO–primed (**A**) and piperacillin-primed (**B**) memory T cell TCR Vβ usage from healthy donors. TCR Vβ subtype expression in naive and drug-primed memory T cells. Data represent mean percentages of T cells expressing the individual TCR Vβ subtypes. Diamonds (◇) indicate skewed TCR Vβ usage, defined as percentage above mean value + 3 SD of TCR Vβ in naive T cells).

$CD45RO^+$ magnetic bead isolation, as previously described. Although some of the obtained memory T cells were used for TCR Vβ FACS analysis, 2×10^6 $CD45RO^+$ T cells were immediately frozen in RNAlater. Naive T cells primed to the β-lactam antibiotic piperacillin (2 mM) were also subjected to TCR Vβ spectratyping analysis and compared with the SMX-NO data.

Generation and characterization of T cell clones

T cell clones were generated from memory and naive T cell priming cultures using previously described methods of serial dilution and subsequent mitogen-driven expansion (23, 24). For testing Ag-specific responses in T cell clones, autologous EBV-transformed B cells were generated as previously described (25) and used as functional APCs. To validate Ag specificity, T cell clones (5×10^4 per well; 96-well plate; total volume, 200 μl) were cultured in duplicate for each experimental condition with irradiated EBV-transformed B cells (1×10^4 per well), with or without SMX-NO (40 μM). After incubation for 48 h (37°C/5% CO_2), [^{3}H]thymidine was added, and cultures were incubated for an additional 16 h before measurement of cellular proliferation by scintillation counting. Clones deemed Ag specific, by obtaining a stimulation index (mean cpm of drug-treated wells/mean cpm of control wells) > 2,

were repetitively stimulated with allogeneic PBMCs (5×10^4 per well; 96-well plate; total volume, 200 μl) in R9 medium supplemented with PHA (5 μg/ml) and IL-2. T cell clone phenotype was assessed using flow cytometry by staining with anti-CTLA4–allophycocyanin or TIM-3–PE. Further assays to determine the SMX-NO–dependent proliferation of T cell clones or the secretion of IFN-γ, IL-13, and granzyme B, with or without PD-L1–, CTLA4–, or TIM-3–blocking Abs, were assessed by [^{3}H]thymidine incorporation and ELISPOT, respectively.

Flow cytometry

A FACSCanto II flow cytometer was used to acquire cells based upon forward/side scatter characteristics. A minimum sample size of 50,000 cells was acquired, and data were analyzed using associated FACSDiva software or Cyflogic software (Cyflo, Turku, Finland).

TCR Vβ analysis by flow cytometry

TCR Vβ protein expression was determined using an IOTest Beta Mark TCR V beta Repertoire Kit (Immunotech, Beckman Coulter). Aliquots of T cells were stained with 24 fluorescence-conjugated TCR Vβ Abs for 20 min in the dark, with further inclusion of CD3-allophycocyanin enabling the gating of T cells. T cells were washed with PBS and resuspended in 300 μl HBSS containing 10% FBS. Data were analyzed using Cyflogic software.

RNA extraction and reverse transcription

Total RNA was extracted from naive and SMX-NO–primed memory T cells (2×10^6) using an RNeasy Mini Kit (Qiagen, Hilden, Germany), following the manufacturer's protocol. After RNA elution from the spin column using RNase-free water, the eluate was passed over the column a second time to increase the RNA concentration. Total RNA was quantified using a NanoDrop ND-8000 spectrophotometer (Thermo Scientific, Runcorn, U.K.), and RNA integrity was assessed using the Agilent Bioanalyzer (Agilent, Cheadle, U.K.). Total RNA (0.4 μg) was reverse transcribed to cDNA using an iScript cDNA Synthesis Kit (Bio-Rad, Deeside, U.K.), as recommended by the manufacturer.

PCR amplification of cDNA

As described previously by Pannetier et al. (26), analysis of CDR3 sizes within the 24 TCR Vβ-chains was performed in a two-step PCR. CDR3 spectratyping was performed. For each sample, aliquots of cDNA (20 ng) were amplified with 1 of 24 Vβ forward primers (10 μM; Metabion, Planegg, Germany) and a Cβ reverse primer (10 μM) using an iCycler thermal cycler (Bio-Rad) and a HotStarTaq Master Mix Kit (Qiagen). The final reaction mix contained 12.5 μl of master mix, 1.3 μl of Vβ forward primer, 1.3 μl of reverse primer, 1 μl of cDNA, and 8.9 μl of RNase-free water. The thermal cycling conditions were as follows: heat activation of Taq polymerase at 95°C for 5 min, followed by 40 cycles of denaturation at 95°C for 45 s, annealing at 60°C for 45 s, extension at 72°C for 1 min, and a final extension step at 72°C for 10 min.

Run-off PCR

PCR products from the first PCR were submitted to three cycles of an elongation run-off reaction with a FAM-labeled Cβ primer (10 μM; Metabion). The final reaction mix contained 0.1 μl of run-off primer, 0.1 μl of PFU polymerase (Promega, Mannheim, Germany), 1 μl of deoxynucleotide triphosphates (30 μM; Promega), 1 μl of 10× PFU buffer (Promega), 1 μl of PCR product, and 6.8 μl of RNase-free water. PCR was performed on an iCycler thermal cycler (Bio-Rad) under the following conditions: 94°C for 2 min, five cycles of 94°C for 25 s, 60°C for 45 s, and 72°C for 45 s, followed by a final elongation step of 72°C for 10 min.

CDR3 spectratyping by GeneScan

Run-off PCR product (2 μl) was added to a mix of Hi-Di Formamide (10 μl) and 500 LIZ size standard (1 μl) in a Thermo-Fast 96 PCR Detection Plate (all from Applied Biosystems, Runcorn, U.K.). The plate was sealed with a 96-well Plate Septa (Applied Biosystems), and the samples were denatured at 94°C for 2 min. CDR3 size was determined using an ABI PRISM 3300 Genetic Analyzer, and data were analyzed using GeneMapper Software Version 4.0 (both from Applied Biosystems).

Statistics

Studies measuring the in vitro proliferation of naive and memory T cells were performed in triplicate cultures and on three or more separate donors. Assays measuring cell proliferation or the secretion of cytokines/cytolytic molecules from SMX-NO–responsive T cell clones were also conducted in triplicate. Data are presented as the mean of the triplicate values with associated SD. A paired *t* test was used for statistical analysis (SigmaPlot 13 software).

Results

TCR Vβ usage of SMX-NO–responsive T cells

Flow cytometry was initially used to explore the comparative TCR Vβ expression between naive T cells and the corresponding SMX-NO–primed memory population. An expansion of the TCR Vβ repertoire was observed in T cells from five donors following in vitro priming to SMX-NO, indicating that clonal expansion of drug-specific T cells had occurred (Table I).

All 24 TCR Vβs could be detected in naive T cells, with mean expression levels ranging from 0.18% for Vβ 9 up to 6.98% for Vβ 2 (Supplemental Table I). After in vitro priming, we observed that, among the responses for the five donors, the expression of up to 16/24 TCR Vβs had increased above that expressed on cells in their naive state (Fig. 1A). Skewing of individual TCR Vβ subtypes was examined, as described by Hashizume et al. (27), who defined skewed TCR Vβ usage as the percentage of a particular TCR Vβ that is above the mean percentage + 3 SD of the same TCR Vβ in normal cells (in this study, naive T cells). Skewed usage of TCR Vβ 4 and 9 was subsequently detected in all five individuals, whereas usage of TCR Vβ 11, 13.6, 14, and 18 was skewed in four donors, and usage of TCR Vβ 5.2 and 5.3 was skewed in three donors (Table II).

The same analysis was conducted on T cells primed against an alternative drug hapten, the β-lactam antibiotic piperacillin. After priming, an increase in the expression of 10 TCR Vβs was observed (Fig. 1B). Skewed usage of TCR Vβ 9 and 13.2 was detected in all three individuals, whereas TCR Vβ 18 and 23 was skewed in two donors, and usage of TCR Vβ 5.3, 13.1, 7.1, 5.1, 1, and 21.3 was seen in one donor.

CDR3 spectratyping analysis of TCR Vβ diversity

The TCR Vβ repertoire of naive and SMX-NO–responsive memory T cells was further analyzed by CDR3 spectratyping. Total RNA from naive and memory T cells was reverse transcribed to cDNA, and TCR Vβ-chain transcripts were amplified prior to analysis on an automated sequencer to determine the CDR3 size pattern of each TCR Vβ subtype. In the absence of antigenic stimulation, CDR3

Table II. Summary of common skewed TCR Vβ usage in SMX-NO–responsive T cells from five healthy donors

TCR Vβ	4	5.2	5.3	9	11	13.6	14	18
S2	●			●	●		●	
S3	●	●	●	●	●	●	●	●
S4	●	●	●	●	●	●	●	●
S5	●	●	●	●	●	●	●	●
S6	●			●		●		●

Black dots denote skewed usage of TCR Vβ.

Table III. Spectratyping analysis of TCR Vβ subtypes with oligoclonal distribution of CDR3 sizes following SMX-NO priming

TCR Vβ	1	2	3	4	5	6A	6BC	7	8	9	11	12	13A	13B	14	15	16	17	18	20	21	22	23	24
S2	●	X		X			●	●		●		●							●					
S3				X	S	S	S		●					●	●				●	●		●		S
S4				X	●					●		●	●	●	●	●			●	X	X			
S5	●	X	S		●			●	S		S		●	●			●	S	●		X		S	
S6	●	X	●	X	●	●	●			●	X		●	●	●		●	●	●		X	●	●	●

S, no sizing data; X, not detected; ●, oligoclonal expansion (oligoclonal distribution of CDR3 lengths defined as skewed Gaussian profile with at least one dominant peak).

profiles of individual TCR Vβs show a Gaussian-like distribution. A distortion of the CDR3 profiles, characterized by the emergence of single or multiple dominant peaks, signifies Ag-specific T cell stimulation leading to clonal expansion. Representative CDR3 spectratyping profiles of skewed TCR Vβs are shown in Supplemental Fig. 1A, 1B. No spectratyping profile could be established for a small number of TCR Vβs, because the genetic analyzer failed to detect the size standard.

Nineteen of twenty-four TCR Vβ subtypes were detected in naive T cells from all five healthy volunteers. As expected, the majority of TCR Vβ spectratyping profiles of naive T cells displayed a polyclonal distribution of CDR3 lengths (defined as quasi-Gaussian profile with at least five peaks). Transcripts of TCR Vβ 2, 4, 11, 20, and 21 were present in some donors but absent in others. In SMX-NO–primed memory T cells, 19/24 TCR Vβ-chains were present in all five donors. TCR Vβ 2, 3, 4, 20, and 21 could only be detected in some of the donors. After SMX-NO priming, up to 80% of TCR Vβ subtypes showed an oligoclonal distribution of CDR3 lengths (skewed Gaussian profile with at least one dominant peak). Skewing of CDR3 profiles from poly- to oligoclonal distribution could be observed for between 6 and 15 TCR Vβs, indicating the expansion of a clonal T cell population reactive to SMX-NO. SMX-NO–specific memory T cells from all five volunteers showed oligoclonal expression of TCR Vβ 18 (Table III). Skewed usage of TCR Vβ 13B was observed in four donors, and TCR Vβ 1, 5, 9, 13A, and 14 displayed a skewed CDR3 pattern in three individuals.

The comparative effect of immune checkpoint receptor blockade between drug Ag–induced naive and memory T cell activation

Following the TCR Vβ analysis, we examined the propensity for coinhibitory pathways to modulate the activation thresholds of these SMX-NO–responsive and, therefore, TCR Vβ–restricted T cell populations. Mature DCs generated from drug-naive donors were cocultured with autologous naive or memory $CD3^+$ T cells in the presence of SMX-NO, with or without PD-L1/CTLA4/TIM-3 block for 8 d. DCs expressed a characteristic phenotype ($CD1a^{negative}$ $CD11a^{high}$ $CD11c^{high}$ $CD14^{negative}$ $CD40^{high}$ $CD83^{low}$ MHC class I^{high} MHC class II^{high}). Importantly, mature DCs also expressed PD-$L1^{high}$ (PD-1 ligand), $CD80^{mid}$ and $CD86^{high}$ (CTLA4 ligands), and galectin-9^{high} (TIM-3 ligand, Supplemental Fig. 1C–E). Upon restimulation, primed naive and memory T cells displayed a dose-dependent proliferative response to SMX-NO (Figs. 2, 3; $*p < 0.05$; SMX-NO, 20–50 μM). For naive T cell priming, blocking PD-L1 and CTLA4 markedly enhanced the proliferative response (Fig. 2) in four of five and six of nine SMX-NO–responsive donors, respectively (Supplemental Table II; $*p < 0.05$). The blockade of CTLA4 resulted in a lesser fold increase in proliferative response (average 2.5-fold increase) than the comparative effect after inclusion of PD-L1 block (average 4.4-fold increase). In contrast to naive T cell priming, blocking PD-L1 had no effect on the proliferation of SMX-NO–exposed memory T cells, whereas inclusion of CTLA4 blockade markedly enhanced the proliferative response in three of six donors (Fig. 3, Supplemental Table III; $*p < 0.05$). Blocking TIM-3 did not enhance the proliferative response of SMX-NO–primed naive or memory T cells from any donor (Figs. 2, 3, Supplemental Tables II and III, respectively).

PD-1, CTLA4, and TIM-3 display discrete expression profiles during drug Ag–induced T cell activation

We previously measured the expression of PD-1 before and during the priming of naive T cells to SMX-NO. PD-1 expression on

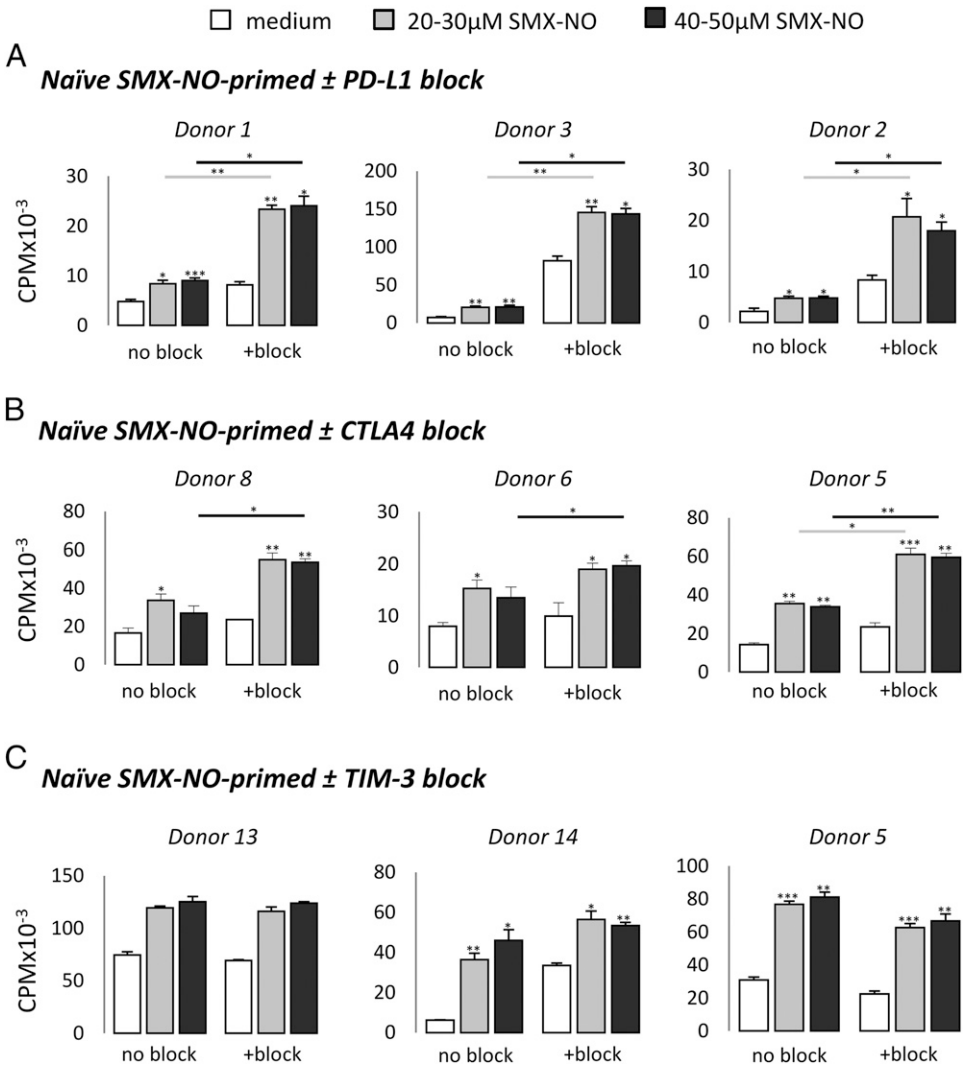

FIGURE 2. Proliferation of SMX-NO–primed naive T cells, with or without coinhibitory receptor-blocking Abs. Naive T cells from healthy donors were cultured with mature autologous monocyte-derived DCs in the presence of SMX-NO (50 μM) for one 1 wk, with or without PD-L1–blocking Abs (5 μg/ml) (**A**), CTLA4-blocking Abs (5 μg/ml) (**B**), or TIM-3–blocking Abs (7.5 μg/ml) (**C**). T cells were harvested and restimulated with fresh mature DCs and SMX-NO (20–50 μM) for 48 h. [^{3}H] Thymidine was added and incubated for an additional 16 h. Data from three representative donors show the mean ± SD of triplicate cultures. Statistical significance denotes a significant increase in the proliferative response compared with medium-only–treated wells within that condition (i.e., TIM-3–blocked cells only). Statistical significance between conditions denotes a significant increase in the proliferative response compared with "no block" wells at a particular drug concentration after normalization of all data values to account for differing basal stimulation. $*p \leq 0.05$, $**p \leq 0.005$, $***p < 0.001$.

CD4$^+$ and CD8$^+$ T cells increased rapidly after priming with SMX-NO. More than 20% of T cells stained positive for 14 d and for 48 h after restimulation of the primed T cells (Fig. 4A). During this investigation, we completed the profiling of PD-1 expression on drug Ag–stimulated memory T cells and similarly assessed the expression kinetics of CTLA4 and TIM-3 on naive and memory T cells.

Although 5–8% of naive T cells expressed CTLA4, the percentage of naive-derived CTLA4$^+$ T cells decreased directly after initial exposure to Ag, before increasing above prestimulation levels by 48 h postrestimulation (Fig. 4B). Although SMX-NO–specific activation of naive T cells increased the percentage of CTLA4$^+$ CD4$^+$ T cells by 2% (8–10%), 6% more (5.3–11.3%) CD8$^+$ T cells expressed CTLA4 after restimulation. TIM-3 expression was also detected on naive T cells; however, in contrast to CTLA4, the percentage of TIM-3$^+$ T cells increased during SMX-NO priming (Fig. 4C). After restimulation, the number of TIM-3$^+$ cells fluctuated before again rising by 72 h postrestimulation so that >50% of naive-derived T cells expressed TIM-3. The maximal increase in TIM-3 expression was similar for CD4$^+$ and CD8$^+$ naive T cells, with a 42.4 and 47.9% increase in comparison with unstimulated naive CD4$^+$ and CD8$^+$ T cells, respectively.

Similar to naive T cells, CTLA4 was expressed on <10% of resting memory T cells (Fig. 4E). In contrast, PD-1 and TIM-3 were expressed on a much higher proportion of quiescent memory T cells (Fig. 4D, 4F, respectively) than naive T cells. The expression kinetics of each receptor during memory T cell stimulation followed those previously observed on naive T cells. Although PD-1 expression increased, peak expression remained <10% greater than basal memory T cell expression. In contrast, peak TIM-3 expression was >45% greater than on quiescent memory T cells. For PD-1 and TIM-3, the increase in receptor expression between naive T cells and that on cells 72 h after restimulation was similar between CD4$^+$ and CD8$^+$ T cell populations (PD-1 expression: CD4$^+$, 9% increase [32.0–41.0%]; CD8$^+$, 7% increase [58.2–65.2%] and TIM-3: CD4$^+$, 48.3% increase [18.6–66.9%]; CD8$^+$, 49.5% increase [21.9–71.4%]). In contrast, as with naive T cell expression, CTLA4 expression on memory T cells was enhanced more on CD8$^+$ T cells (7.3% [3.1–10.4%]) than on CD4$^+$ T cells (1.5% [7.7–9.2%]) (Fig. 4E).

The expression of CTLA4 and TIM-3 is enhanced on drug Ag–primed dividing T cells

The high expression of coinhibitory receptors has previously been associated with T cell exhaustion. In our previous investigation, we identified that PD-1 was expressed on dividing T cells and, therefore, was not individually a marker of exhaustion. We again questioned this association for CTLA4 and TIM-3 by performing a detailed analysis of SMX-NO–primed naive T cell proliferation by costaining cells with CFSE. CTLA4 was expressed on a significant proportion of CD4$^+$ (15.1%) and CD8$^+$ (10.7%) dividing T cells, both of which represented greater proportions compared

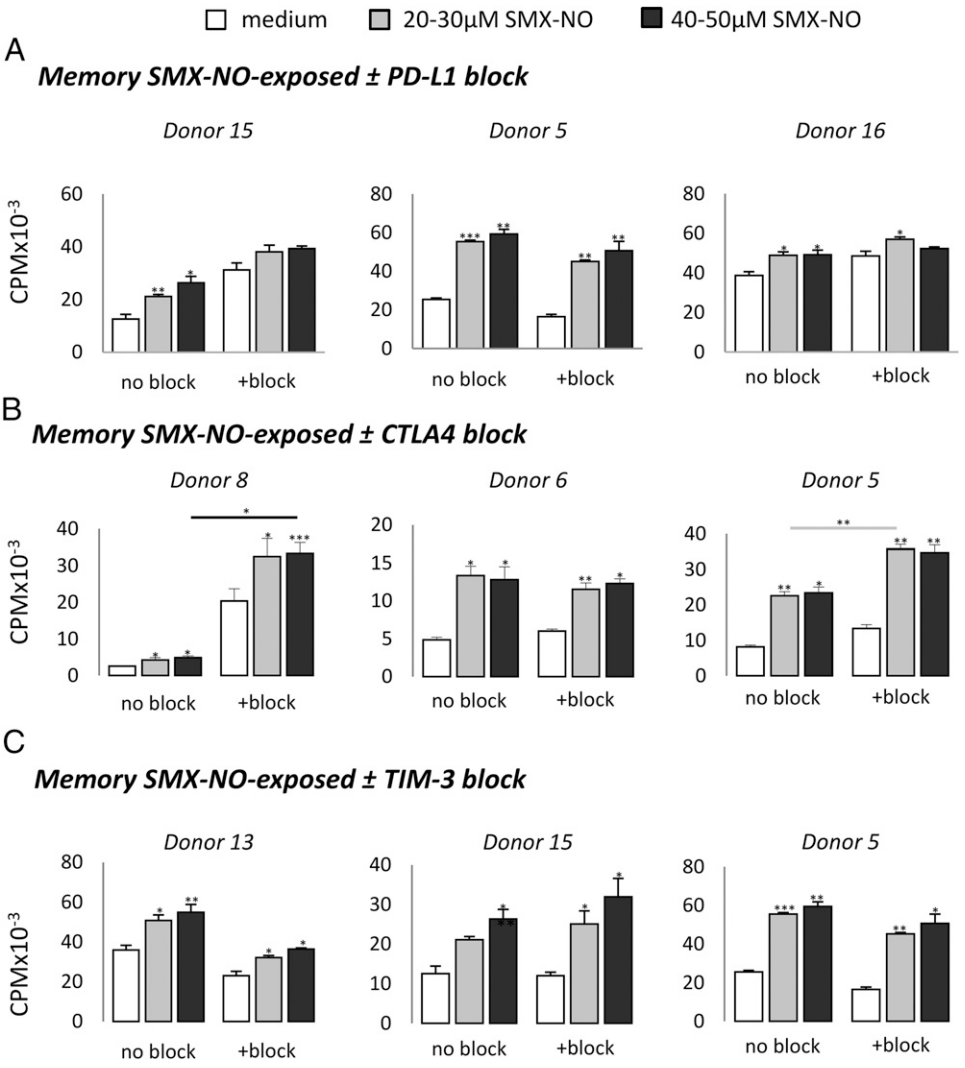

FIGURE 3. Proliferation of SMX-NO–exposed memory T cells, with or without coinhibitory receptor-blocking Abs. Memory T cells from healthy donors were cultured with mature autologous monocyte-derived DCs in the presence of SMX-NO (50 μM) for one 1 wk, with or without PD-L1–blocking Abs (5 μg/ml) (**A**), CTLA4-blocking Abs (5 μg/ml) (**B**), or TIM-3–blocking Abs (7.5 μg/ml) (**C**). T cells were harvested and restimulated with fresh mature DCs and SMX-NO (20–50 μM) for 48 h. [^{3}H]Thymidine was added and incubated for an additional 16 h. Data from three representative donors show the mean ± SD of triplicate cultures. Statistical significance denotes a significant increase in the proliferative response compared with medium-only–treated wells within that condition (i.e., TIM-3–blocked cells only). Statistical significance between conditions denotes a significant increase in the proliferative response compared with "no block" wells at a particular drug concentration after normalization of all data values to account for differing basal stimulation. $*p \leq 0.05$, $**p \leq 0.005$, $***p < 0.001$.

with CTLA4 expression on the corresponding nondividing T cell populations (Fig. 5A). Similarly, TIM-3 expression was found on 5- and 3-fold more dividing CD4$^+$ and CD8$^+$ T cells, respectively, compared with those in a quiescent state (Fig. 5B).

The expression level of individual coinhibitory receptors has no effect on the response of drug Ag–responsive T cell clones

In comparison with the modest 4-fold difference in PD-1 expression previously reported between T cell clones, flow cytometric analysis of 40 representative SMX-NO–specific T cell clones revealed a >27-fold difference in CTLA4 expression and a >10-fold difference in TIM-3 surface expression (Fig. 6A). We previously reported that the degree of PD-1 expression had no effect on T cell clone activity. Despite a much greater variation in the expression of CTLA4 and TIM-3 between T cell clones, the level of expression of these coinhibitory receptors did not affect the proliferative response of each clone (Fig. 6B). Although the clone with the highest TIM-3 expression (clone 49) was also the clone with the highest stimulation index, the stimulation index of the other three clones (clones 71, 26, 97) showed no correlation with TIM-3 expression. For example, clone 71 had a similar stimulation index to that of clone 97 but only one third of the TIM-3 surface expression.

We then measured the surface expression of CTLA4 and TIM-3 on clones over a period of 10 d, with and without SMX-NO stimulation. Although staining over a similar time period had shown relatively stable PD-1 expression, the expression profile for CTLA4 and TIM-3 was more varied (Fig. 6C). In the absence of Ag, the expression of both receptors remained relatively constant over a period of 240 h. In the presence of SMX-NO, the expression of CTLA4 and TIM-3 increased above that of basal levels in clone 1 (CTLA4) and clones 3 and 4 (TIM-3). For clone 1, maximal CTLA4 expression was observed at 120 h, at which point expression on SMX-NO–stimulated wells was >2.5-fold higher than prior to SMX-NO exposure (0-h mean fluorescence intensity [MFI]: 136, 120-h MFI: 358) and >3-fold greater than the expression at the same time point on cells not treated with Ag (untreated cells 120-h MFI: 115). Both clones analyzed for TIM-3 expression showed maximal expression at 48 h post–SMX-NO exposure. At this time point, expression of TIM-3 on SMX-NO–stimulated cells was >10-fold and >2-fold higher than on cells prior to SMX-NO exposure for clones 3 and 4, respectively (clone 3: 0-h MFI, 262; 48-h MFI, 2626; clone 4: 0-h MFI, 458; 48-h MFI, 936) and >13.5-fold and >5.5-fold greater than the expression of cells not treated with Ag (untreated cells 120-h MFI: clone 3, 192; clone 4, 168) at a similar time point.

PD-L1, CTLA4, and TIM-3 have no effect on the effector response of SMX-NO–responsive T cell clones

To further assess the role of immune checkpoint receptors in the regulation of secondary T cell responses, we explored the roles of CTLA4 and TIM-3 on SMX-NO–specific T cell clones generated

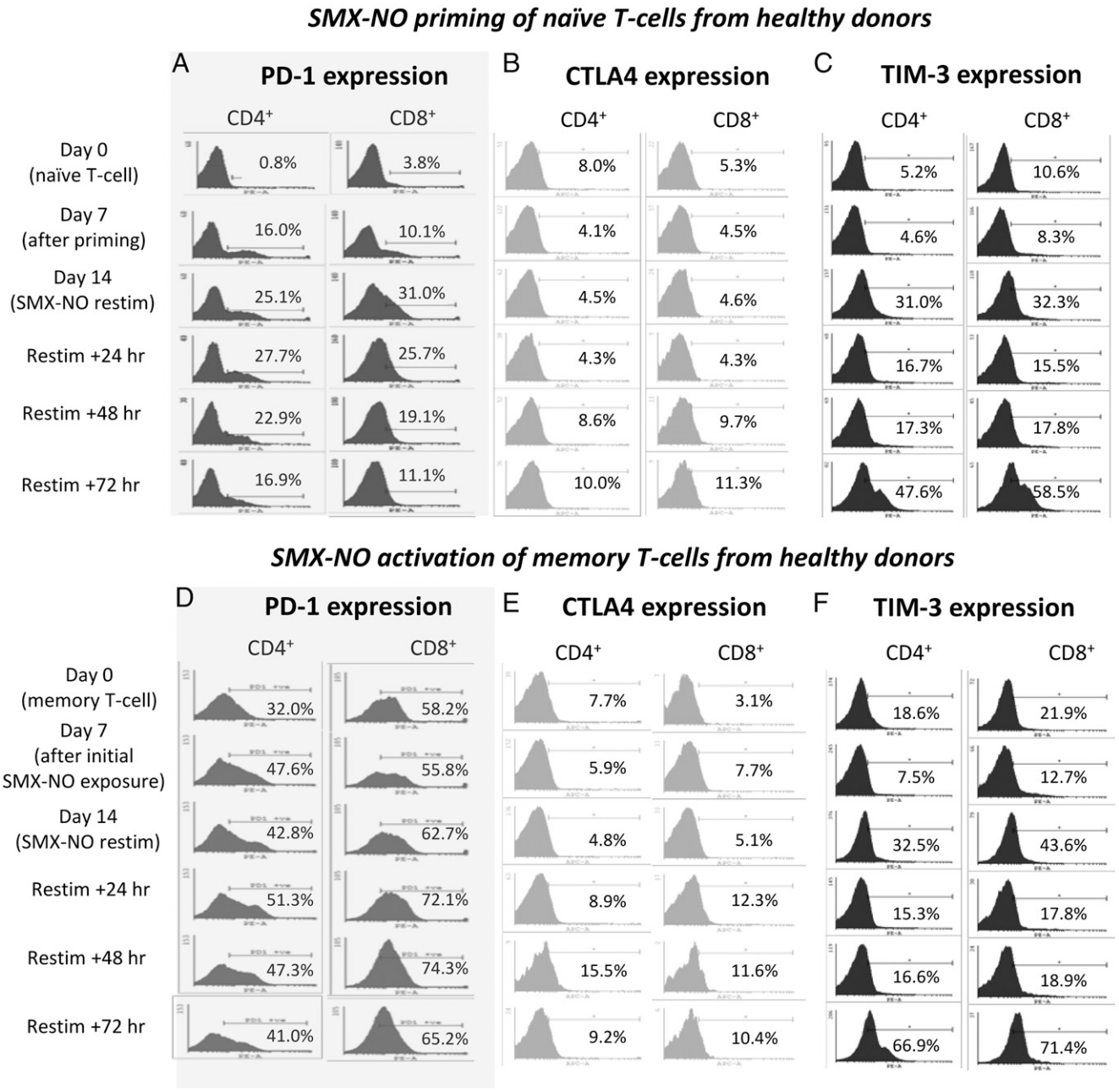

FIGURE 4. Coinhibitory receptor expression during the SMX-NO–specific activation of $CD4^+$ and $CD8^+$ naive and memory T cells from healthy donors. Expression of coinhibitory receptors on naive [PD-1 (**A**), CTLA4 (**B**), TIM-3 (**C**)] or memory T cells [PD-1 (**D**), CTLA4 (**E**), TIM-3 (**F**)] from healthy donors during stimulation and during restimulation with SMX-NO (50 μM) using mature autologous DCs. Samples of T cells were harvested at various time points and labeled with CD4, CD8, and PD-1/CTLA4/TIM-3 fluorochrome-bound Abs. Percentages indicate the proportion of cells that stain positive for each coinhibitory receptor.

from healthy donor–primed naive T cells, because previous work had shown that PD-L1 block led to a modest increase in cytokine secretion from T cell clones. The proliferative capacity and the ability to secrete cytokines and cytolytic molecules in the presence of SMX-NO were assessed on six representative T cell clones, with and without CTLA4 or TIM-3 blockade (Fig. 7A, 7B, respectively). All clones proliferated significantly in the presence of SMX-NO ($*p < 0.005$), and the addition of CTLA4- or TIM-3–blocking Ab did not significantly increase the proliferative response or the secretion of IFN-γ, IL-13, or granzyme B in response to SMX-NO for any of the six T cell clones. The inability of CTLA4 and TIM-3 to regulate the responses of T cell clones reflects the reduced capacity of such pathways to control secondary (memory) responses, especially when every cell has specificity for the drug, in comparison with the initial priming response.

$CD25^+$ T cells (Tregs) effectively dampen SMX-NO–induced naive and memory T cell activation

The Treg population was selectively removed from the T cell population using $CD25^+$ as a marker for these cells. To determine the scale of regulation imposed by $CD25^+$ Tregs on drug Ag–induced immune activation, we seeded autologous $CD25^+$ T cells into the coculture. As the yield of T cells varied between donors, not all conditions (i.e., addition of 600,000 Tregs) could be performed for donors from whom we isolated a smaller number of

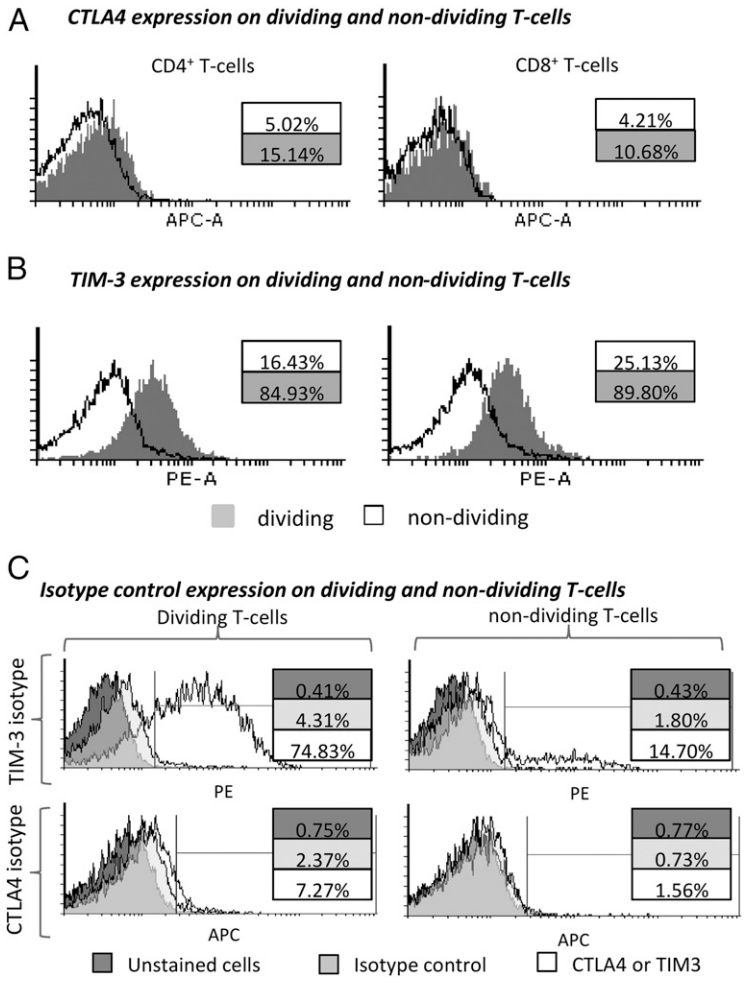

FIGURE 5. Expression of CTLA4 and TIM-3 on dividing and nondividing T cells derived from priming healthy donor naive T cells to SMX-NO. Naive T cells from healthy donors were cultured with mature autologous DCs in the presence of SMX-NO (50 μM) for 1 wk. T cells were stained with CFSE and restimulated with fresh mature DCs and SMX-NO (50 μM) for 72 h. T cells were incubated with CTLA4-allophycocyanin or TIM-3–PE, and with CD4- and CD8-specific fluorochromes. Expression of CTLA4 (**A**) and TIM-3 (**B**) on $CD4^+$ or $CD8^+$ T cell populations separately (shaded graph, expression on dividing T cells; black line, expression on nondividing T cells). Percentages indicate the percentage of each population gated positive for each coinhibitory receptor. (**C**) Comparative expression on both dividing and nondividing T cell populations of the respective isotype (IgG1) control Abs for CTLA4 or TIM-3 (dark gray shaded graph, unstained expression; light gray shaded graph, expression of isotype control; black line, expression of CTLA4 or TIM-3).

Tregs. For these donors we utilized all available Tregs using the most suitable conditions (i.e., additions of only 200,000 and 400,000 Tregs). The addition of 2×10^5 $CD25^+$ T cells led to a significant reduction in the drug Ag–induced proliferation of naive- and memory-derived T cells from all donors (Fig. 8A, 8B, respectively). A similar trend was observed upon analysis of IFN-γ and IL-13 secretion from naive- and memory-derived cells (Fig. 9A, 9B, respectively). Increasing the number of $CD25^+$ T cells further reduced the SMX-NO–specific response. These functionally suppressive Tregs expressed coinhibitory receptors and ligands, as determined by flow cytometry (Fig. 8C).

Discussion

The association of specific HLA alleles with drug hypersensitivity enticed the scientific community to reinvestigate the role of T cells in this form of iatrogenic disease. However, for the vast majority of drugs, HLA allele associations have not been identified or do not solely account for the onset of a reaction (28). Therefore, it is apparent that predisposition to hypersensitivity is seldom simplistic and/or mediated by singular genetic traits but is more frequently facilitated by a combination of susceptibility factors.

Three key areas have the potential to influence drug Ag–induced T cell activation. First, Ko et al. (7) demonstrated the importance of investigating both sides of the MHC–TCR interaction, because they found that the use of specific TCR Vβs alongside HLA-B*15:02 is required for hypersensitivity to the antiepileptic drug CBZ. Second, multiple studies have identified that dysregulated coinhibitory receptors involved in T cell activation can propagate autoimmunity (29–35) and that blocking these pathways in cancer models can significantly enhance functional T cell responses (14, 36, 37). Thus, it is conceivable that dysregulated regulatory pathways may contribute to the inadvertent activation of T cells to drug Ags. Third, it has been reported that Tregs can prevent TEN-associated epidermal injury in model systems, highlighting that susceptibility in patients may be linked to a defect in normal Treg function (16, 17). We are interested in examining these factors within a single model system. Using the drug Ag SMX-NO, for which HLA associations have not been identified (38), we have investigated the role of specific TCR Vβ subtypes, immune checkpoint signaling, and Tregs during drug Ag–induced T cell activation.

To assess the role of individual TCR subtypes during drug Ag–specific T cell responses, we explored the TCR Vβ repertoire of T cells before and after SMX-NO priming. The successful priming of naive T cells from all donors was confirmed by proliferation analysis in response to SMX-NO. To profile TCR Vβ usage, we analyzed protein expression by flow cytometry, as well as mRNA expression using molecular CDR3 spectratyping, because both techniques have been widely used across different disease settings (39–42). SMX-NO–primed T cells displayed broad TCR Vβ usage, with increased expression levels in up to 16 TCR Vβs. Skewing was observed for nine Vβ subtypes across the five donors, indicating that multiple TCRs may be involved in drug Ag recognition. Given that SMX-NO is known to modify a range of cellular proteins and that protein adducts stimulate T cells from hypersensitive patients (24, 43–45), the observation that multiple TCRs are activated was anticipated. Furthermore, common

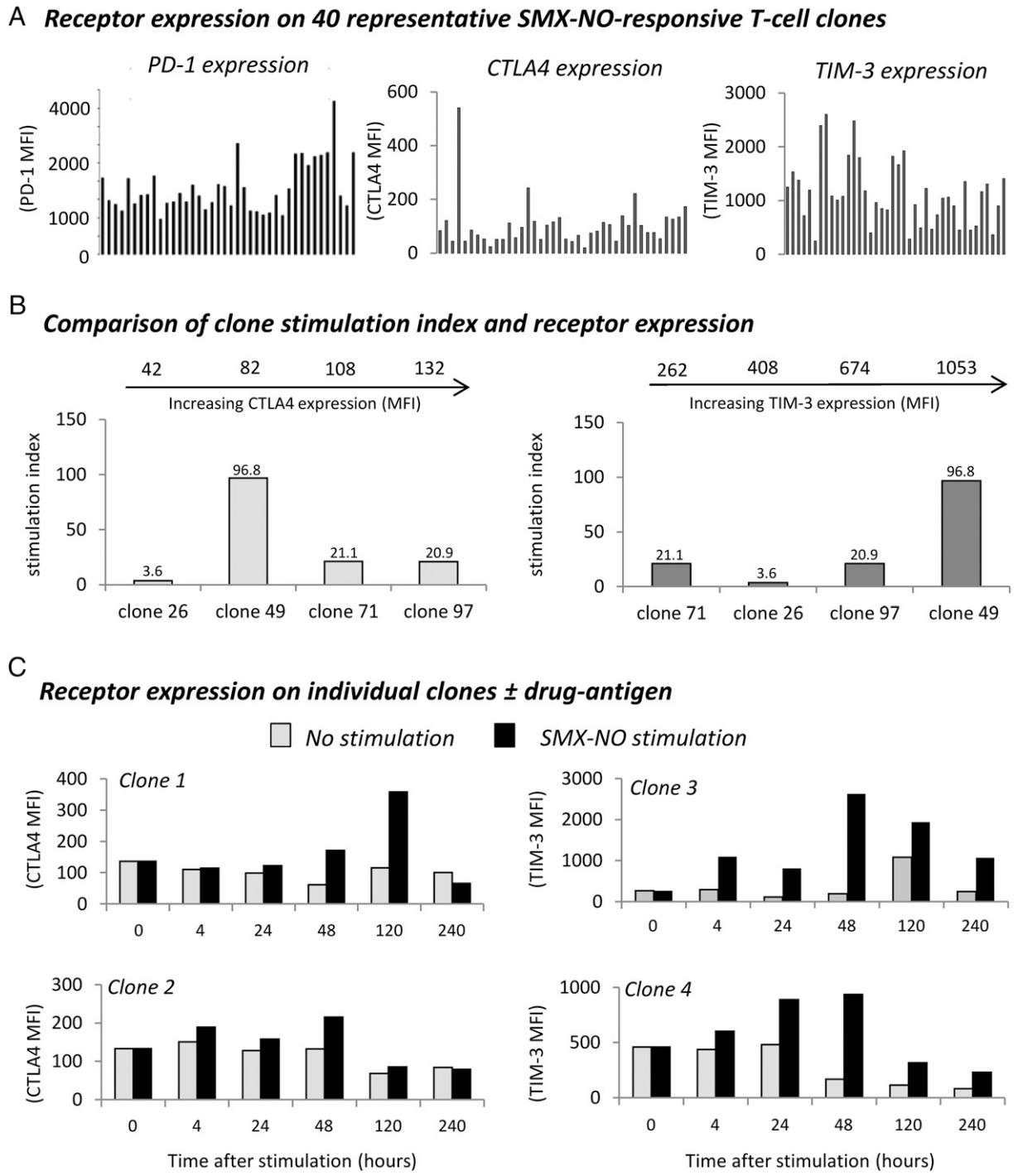

FIGURE 6. Expression–activity relationship of CTLA4 and TIM-3 on SMX-NO–responsive T cell clones. (**A**) Expression of PD-1, CTLA4, and TIM-3 on 40 representative T cell clones derived from priming healthy donor naive T cells to SMX-NO. (**B**) The proliferative response of T cell clones expressing varied levels of CTLA4 or TIM-3 in response to SMX-NO stimulation, as measured by [^{3}H]thymidine incorporation. The MFI derived from flow cytometry, indicating the relative expression of CTLA4 or TIM-3, is shown for each clone at the top of the graphs. (**C**) Expression of CTLA4 and TIM-3 on representative T cell clones over 240 h, with or without SMX-NO stimulation (40 μM).

skewing of particular TCR Vβ subtypes (Vβ 4 and Vβ 9) in all drug-responsive individuals indicates that a public TCR repertoire may be involved in recognition of SMX-NO–derived Ags. Similar observations were made in this study with the β-lactam antibiotic piperacillin, which forms protein adducts through the covalent modification of lysine residues, and elsewhere with abacavir, in which case the extensive TCR usage is thought to be responsible for the recognition of diverse novel self-peptides presented on HLA-B*57:01 in the presence of abacavir (8).

Detailed mRNA analysis using CDR3 spectratyping showed that 11 TCR Vβ subtypes were present in both naive and SMX-NO–specific T cells from all volunteers, whereas 6 TCR Vβs (2–4, 11, 20, 21) were only detected in some donors. In naive T cells, most TCRs displayed polyclonal CDR3 patterns, whereas CDR3 profiles of SMX-NO–specific T cells showed oligoclonal expansions in up to 16 Vβ subtypes. CDR3 spectra only partially match the results obtained by flow cytometry, which is likely due to the enhanced sensitivity of CDR3 spectratyping, and the failed am-

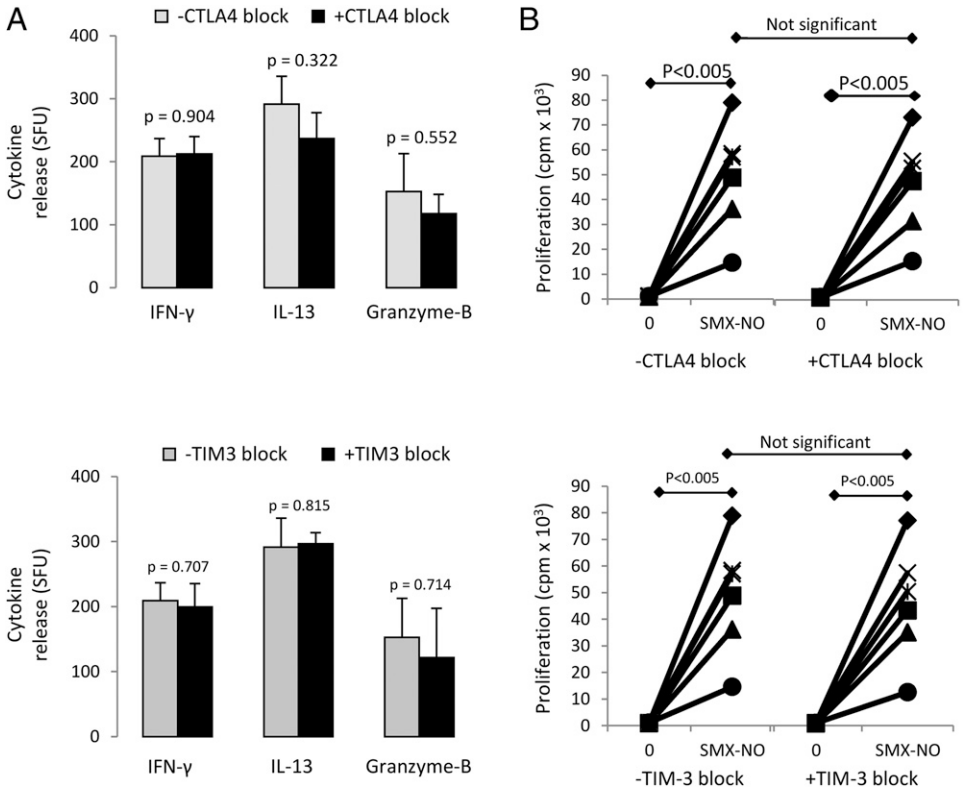

FIGURE 7. Activation of SMX-NO–responsive T cell clones, with or without coinhibitory receptor blockade. Secretion of IFN-γ, IL-13, and granzyme B (**A**) and the proliferative response of T cell clones in response to SMX-NO stimulation (**B**), with or without anti-CTLA4 (10 μg/ml) or anti–TIM-3 (7.5 μg/ml) treatment. Cytokine secretion was measured by ELISPOT, and proliferative analysis was by [^{3}H]thymidine incorporation. Statistical significance between conditions denotes a significant increase/decrease in proliferative response or cytokine release.

plification of specific TCR Vβ transcripts due to inadequate binding specificities of certain Vβ primers. Despite this, common skewing of particular TCR Vβ subtypes was observed between the two techniques. For spectratyping analysis, skewing was observed for TCR Vβ 18 in five of five donors, for TCR Vβ 13B in four of five donors, and for TCR Vβ 1, 5, 9, 13A, and 14 in three of five volunteers. These findings strengthen the proposal that T cell responses to SMX-NO–derived Ags may be controlled by public TCRs, which are present in all responsive individuals, alongside private TCR repertoires specific to each individual.

While the TCR Vβ analysis builds toward a full characterization of the role of signal 1 during SMX-NO–induced T cell activation, the role of signal 2 on the resultant Ag-specific and TCR Vβ–restricted T cells remains largely undefined. An in vitro T cell assay was subsequently used to block individual immune checkpoints to "peel away" and reveal the influence of individual layers of regulation, as well as to assess the kinetics of coinhibitory receptor expression during the drug Ag–specific activation of naive or memory T cells. This work builds upon our previously published work exploring the effects of PD-1 on SMX-NO–induced T cell activation (46) and expands further to similarly detail the function of the CTLA4 and TIM-3 receptor pathways. We identified an enhanced proliferative T cell response after priming naive T cells to SMX-NO in the presence of PD-L1– and CTLA4-blocking Abs. PD-L1 block had a greater regulatory role during primary T cell responses to SMX-NO, with an average 4.4-fold increase in the proliferative response compared with a 2.5-fold increase for CTLA4 block. These data agree with the work of Parry et al. (47), who studied T cell activation–induced gene transcripts and found that the generation of just 67% of transcripts was hindered by CTLA4 ligation compared with 90% upon PD-1 activation. In contrast, we detected no significant increase with the inclusion of TIM-3 block. The apparent lack of regulation by TIM-3 may be related, in part, to its more restricted expression profile compared with CTLA4 and PD-1 (expressed on all T cells) (48, 49). Because the characterization of TIM-3 has been largely performed using mice, it may be that there are functional discrepancies between human and mouse TIM-3.

Lucas et al. (9) recently described the ability of drug-derived Ags to stimulate memory T cells from drug-naive donors via heterologous immunity. Thus, when considering the onset of hypersensitivity, it is necessary to evaluate the role of immune checkpoints during primary and secondary T cell responses. Using our in vitro assay, and in complete contrast to naive T cell priming, memory T cell responses to SMX-NO were not enhanced by the blockade of PD-L1. Similarly, blocking TIM-3 did not increase the memory T cell response. In contrast, blocking CTLA4 enhanced memory drug Ag–specific responses; however, it did so in a smaller proportion of donors (three of six) compared with primary T cell responses. As expected, our data describe a greater role for coinhibitory regulation during primary, rather than secondary, T cell responses, in line with the more stringent requirements and higher activation thresholds for the activation of naive T cells. The requirement for additional signaling minimizes the risk for a naive T cell response to nonharmful or self-antigen, a requirement that is unnecessary for memory T cells as a result of their predefined Ag specificity.

We further examined the dynamics of coinhibitory receptor expression on naive and memory T cells during T cell activation. The percentage of PD-1$^+$ memory cells increased greatly after initial Ag stimulation, peaking shortly after restimulation in a similar manner to that described on naive T cells (46). CTLA4 expression on naive T cells has been shown to be low and inducible upon activation (50), whereas the TIM-3 profiles of CD4$^+$ and CD8$^+$ T cells are less well defined. Hastings et al. (51) found that TIM-3 expression was generally restricted to CD4$^+$ T cells, which were only found in human lymph nodes, with peripheral CD4$^+$ T cells showing little expression until induced poststimulation. Although we found that exposure of naive T cells to SMX-NO did not initially enhance CTLA4 expression, in line with

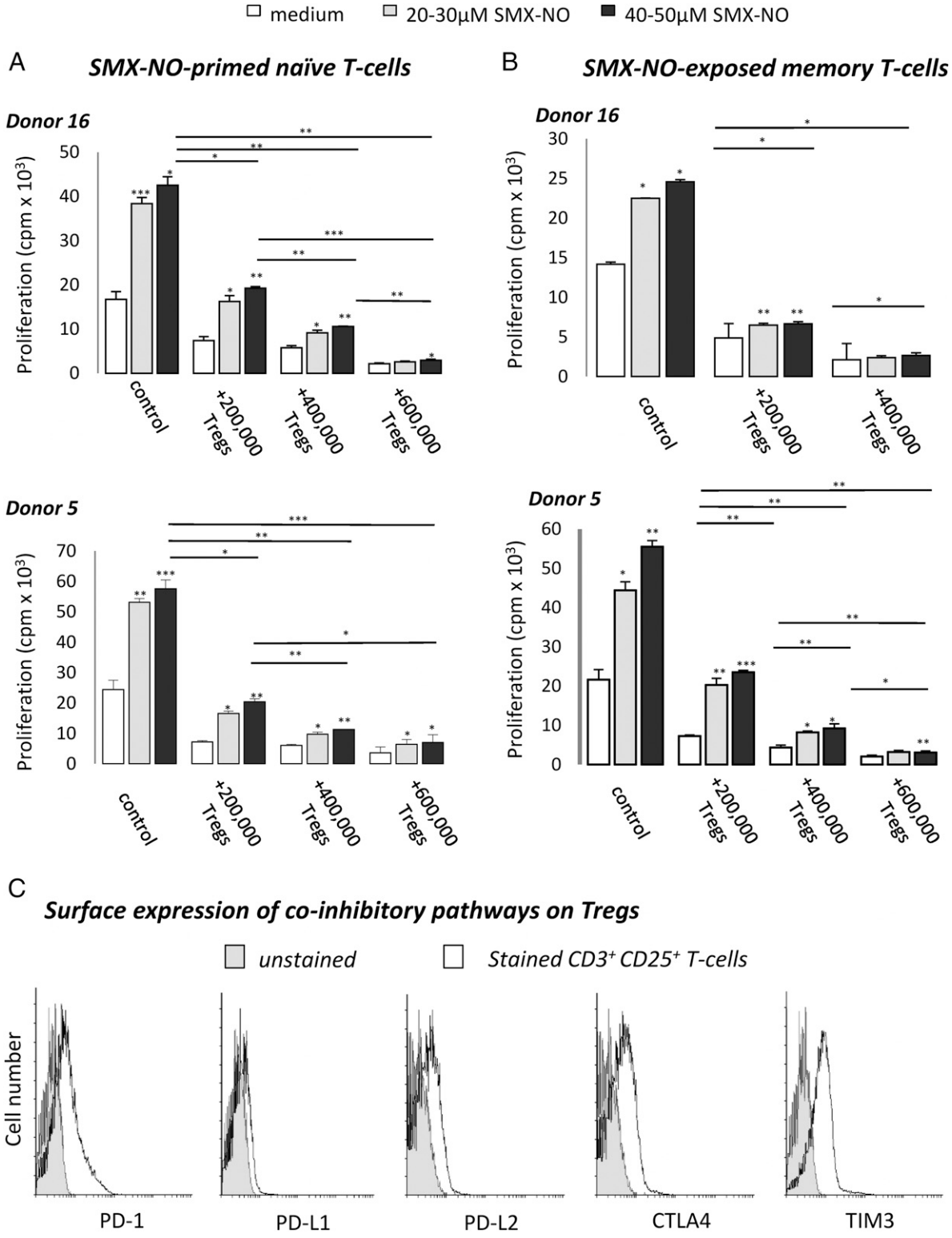

FIGURE 8. Suppressive effect of autologous $CD25^+$ Tregs on the SMX-NO–induced activation of naive and memory T cells from healthy donors. Naive (**A**) or memory (**B**) T cells were cultured with mature DCs and SMX-NO (50 μM) for 1 wk, with or without autologous $CD25^+$ Tregs ($2–6 \times 10^5$ per well). T cells were harvested and restimulated with fresh mature DCs and SMX-NO (20–50 μM) for 48 h before measurement of proliferative capacity through the incorporation of [^{3}H]thymidine. (**C**) Expression of PD-1, PD-L1, PD-L2, CTLA4, and TIM-3 on autologous Tregs was analyzed by flow cytometry to identify the propensity for coinhibitory pathways to aid Treg-mediated suppression of SMX-NO–induced T cell responses. Statistical significance between conditions denotes a significant increase/decrease in proliferative response. $*p \leq 0.05$, $**p \leq 0.005$, $***p < 0.001$.

previous reports citing an increase after 2–3 d (52), we observed a slight increase in the percentage of naive T cells expressing CTLA4 between 48 and 72 h after restimulation with SMX-NO. CTLA4 expression on memory T cells was enhanced similarly after restimulation. The proportion of naive and memory $TIM\text{-}3^+$ cells decreased after initial Ag exposure and restimulation but increased toward the end of both the initial culture with Ag (priming) and after reexposure (restimulation). This pattern is

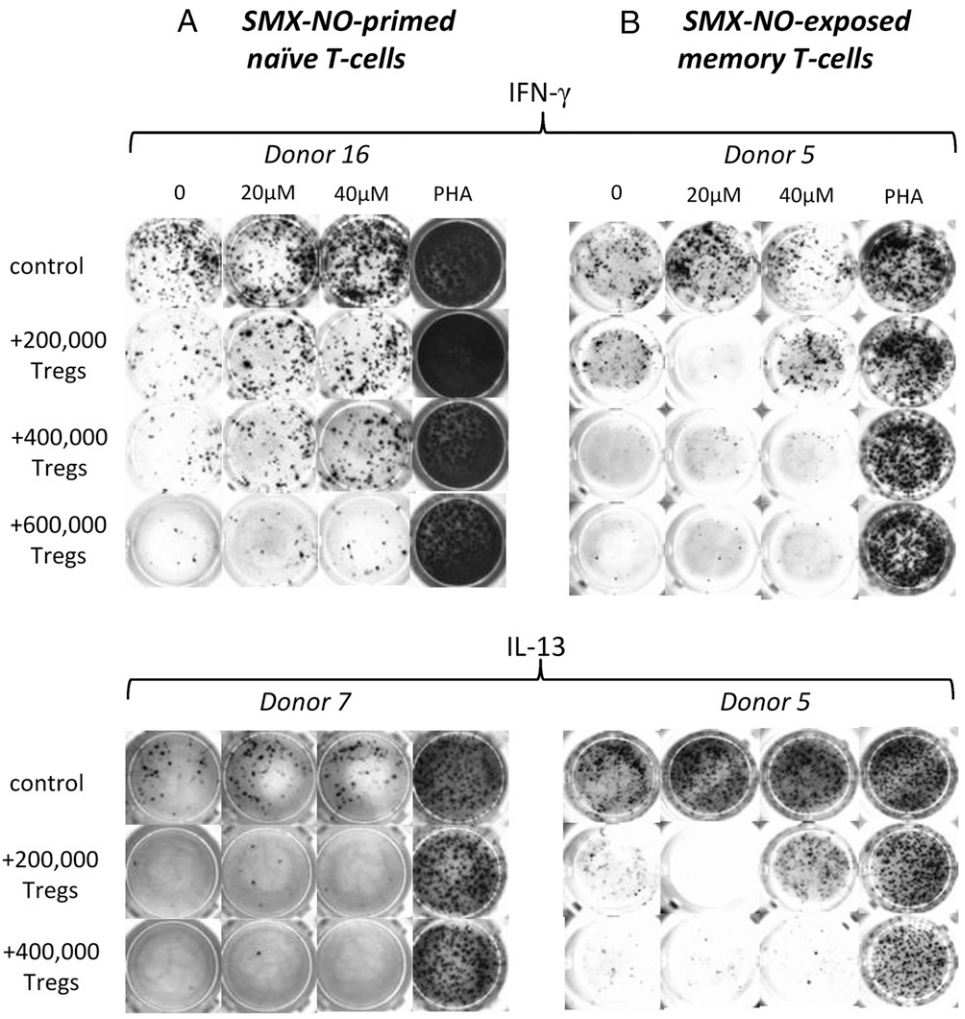

FIGURE 9. Quantitative effect of $CD25^+$ Treg–mediated inhibition of cytokine secretion on drug Ag–mediated T cell activation. Secretion of IFN-γ and IL-13 after SMX-NO–induced activation of 2.5×10^6 naive (**A**) or memory (**B**) T cells from healthy donors, with or without 2–6×10^5 $CD25^+$ Tregs per well. Autologous Tregs were removed from the control naive and memory T cell populations. Tregs were supplemented back into the assays prior to addition of the drug Ag.

likely used to promote a strong initial response by reducing expression before increasing it at later time points to prevent a long-lasting potentially damaging response. This timeline is supported by two previous observations regarding the TIM-3 ligand, galectin-9. First, galectin-9 expression is downregulated in the lymph nodes after immune activation, which is thought to allow the initial generation of a Th1 response (48). Second, the subsequent expansion of Th1 T cells results in IFN-γ secretion, which, in turn, upregulates galectin-9 in a negative-feedback loop to prevent a runaway immune response (53). In naive and memory cultures, the percentage of $TIM\text{-}3^+$ cells increased by a similar amount upon Ag stimulation for $CD4^+$ and $CD8^+$ T cell populations, indicating that TIM-3 regulates all responsive T cells equally during a drug-derived Ag-specific response. The expression profiles of PD-1, CTLA4, and TIM-3 paint a complex picture of regulation, with different receptors regulating different phases of a response. Specifically, these data show that PD-1 expression is increased soon after T cell activation and so likely has a more prominent role in regulation during the initial encounter of T cells with Ag. In contrast, TIM-3 and CTLA4 may play a more prominent role during late-stage T cell responses.

Because coinhibitory pathways can function to prevent T cell stimulation, multiple studies have linked the high expression of specific coinhibitory receptors to an exhausted T cell phenotype: a quiescent state characterized by an inability to proliferate and produce cytokines (54). Previously, we reported that a high proportion of dividing SMX-NO–specific T cells were $PD\text{-}1^+$; thus, PD-1 does not represent a unique marker for exhaustion. However, similar investigations have not been performed for CTLA4 and TIM-3. Indeed, assessment of the functionality of $PD\text{-}1^+$ $TIM\text{-}3^+$ tumor-infiltrating T cells found that these cells represented an exhausted phenotype, whereas other studies reported that TIM-3 expression can identify exhausted T cells in patients with HIV or hepatitis C virus infection (55, 56). Upon analysis of $CD4^+$ and $CD8^+$ T cells, we found that a significant proportion of actively proliferating cells expressed CTLA4 or TIM-3, as quantified by CFSE incorporation. In all instances, the proportion of dividing T cells expressing either receptor was greater than the comparative proportion of nondividing T cells. Because up to seven different coinhibitory receptors are expressed on functionally exhausted T cells during chronic infection (57), our data highlight the importance of not singling out individual receptors as markers of T cell exhaustion. Moreover, using T cell clones, we demonstrate that the level of CTLA4 or TIM-3 expression can vary widely among autologous Ag-responsive cells. Importantly, the level of expression did not correlate strongly with the strength of the SMX-NO–specific T cell responses.

Finally, we explored the inhibitory effect of Tregs that expressed PD-L1, PD-L2, CTLA-4, and Tim-3 by reintroducing autologous $CD25^+$ T cells into the priming culture in incremental quantities (200,000, 400,000, or 600,000 Tregs). The stimulation of naive and memory T cell responses was dampened by the addition of Tregs and that suppression was increased with the addition of more Tregs. Further work should investigate whether Treg-mediated

suppression of drug-specific T cells is regulated by coinhibitory receptor signaling and/or the secretion of suppressive cytokines.

In summary, we have successfully used an in vitro model to highlight the propensity for various non-HLA risk factors to enhance the likelihood of drug Ag–induced T cell activation. We show that T cell responses to SMX-NO are dependent on the availability of specific TCR Vβ repertoires and that these Ag-responsive T cells are highly regulated by coinhibitory mechanisms that can be enforced by resident Tregs. Our report demonstrates that an individual may be predisposed to develop hypersensitivity by distinct TCR Vβ subtypes that form private and public repertoires; dysregulation of the PD-1 or CTLA4 pathways, which predominantly control naive and memory T cell responses, respectively; or a lack of functional Tregs as autologous $CD25^+$ Tregs, which can effectively suppress effector naive and memory T cell responses at a 1:5 ratio. Until recently, many of these factors have been overlooked due to strong interest in the role of HLA interactions. Although these associations remain important, it is highly likely that the exploration of other risk factors will be required to fully define individual predisposition to drug hypersensitivity.

Acknowledgments

We thank the volunteers for their generous blood donations.

Disclosures

The authors have no financial conflicts of interest.

References

1. Holt, M. P., and C. Ju. 2006. Mechanisms of drug-induced liver injury. *AAPS J.* 8: E48–E54.
2. Meng, X., R. E. Jenkins, N. G. Berry, J. L. Maggs, J. Farrell, C. S. Lane, A. V. Stachulski, N. S. French, D. J. Naisbitt, M. Pirmohamed, and B. K. Park. 2011. Direct evidence for the formation of diastereoisomeric benzylpenicilloyl haptens from benzylpenicillin and benzylpenicillenic acid in patients. *J. Pharmacol. Exp. Ther.* 338: 841–849.
3. Nhim, C., S. Delluc, F. Halgand, L. de Chaisemartin, R. J. Weaver, N. Claude, D. Joseph, B. Maillère, and M. Pallardy. 2013. Identification and frequency of circulating CD4(+) T lymphocytes specific to benzylpenicillin in healthy donors. *Allergy* 68: 899–905.
4. Chung, W.-H., S.-I. Hung, H.-S. Hong, M.-S. Hsih, L.-C. Yang, H.-C. Ho, J.-Y. Wu, and Y.-T. Chen. 2004. Medical genetics: a marker for Stevens-Johnson syndrome. *Nature* 428: 486.
5. Mallal, S., D. Nolan, C. Witt, G. Masel, A. M. Martin, C. Moore, D. Sayer, A. Castley, C. Mamotte, D. Maxwell, et al. 2002. Association between presence of HLA-B*5701, HLA-DR7, and HLA-DQ3 and hypersensitivity to HIV-1 reverse-transcriptase inhibitor abacavir. *Lancet* 359: 727–732.
6. Martin, M. A., T. E. Klein, B. J. Dong, M. Pirmohamed, D. W. Haas, and D. L. Kroetz, Clinical Pharmacogenetics Implementation Consortium. 2012. Clinical pharmacogenetics implementation consortium guidelines for HLA-B genotype and abacavir dosing. *Clin. Pharmacol. Ther.* 91: 734–738.
7. Ko, T.-M., W.-H. Chung, C.-Y. Wei, H.-Y. Shih, J.-K. Chen, C.-H. Lin, Y.-T. Chen, and S.-I. Hung. 2011. Shared and restricted T-cell receptor use is crucial for carbamazepine-induced Stevens-Johnson syndrome. *J. Allergy Clin. Immunol.* 128: 1266–1276.e11.
8. Illing, P. T., J. P. Vivian, N. L. Dudek, L. Kostenko, Z. Chen, M. Bharadwaj, J. J. Miles, L. Kjer-Nielsen, S. Gras, N. A. Williamson, et al. 2012. Immune self-reactivity triggered by drug-modified HLA-peptide repertoire. *Nature* 486: 554–558.
9. Lucas, A., M. Lucas, A. Strhyn, N. M. Keane, E. McKinnon, R. Pavlos, E. M. Moran, V. Meyer-Pannwitt, S. Gaudieri, L. D'Orsogna, et al. 2015. Abacavir-reactive memory T cells are present in drug naïve individuals. *PLoS One* 10: e0117160.
10. Waterhouse, P., J. M. Penninger, E. Timms, A. Wakeham, A. Shahinian, K. P. Lee, C. B. Thompson, H. Griesser, and T. W. Mak. 1995. Lymphoproliferative disorders with early lethality in mice deficient in Ctla-4. *Science* 270: 985–988.
11. Nishimura, H., T. Okazaki, Y. Tanaka, K. Nakatani, M. Hara, A. Matsumori, S. Sasayama, A. Mizoguchi, H. Hiai, N. Minato, and T. Honjo. 2001. Autoimmune dilated cardiomyopathy in PD-1 receptor-deficient mice. *Science* 291: 319–322.
12. Tivol, E. A., F. Borriello, A. N. Schweitzer, W. P. Lynch, J. A. Bluestone, and A. H. Sharpe. 1995. Loss of CTLA-4 leads to massive lymphoproliferation and fatal multiorgan tissue destruction, revealing a critical negative regulatory role of CTLA-4. *Immunity* 3: 541–547.
13. Teft, W. A., M. G. Kirchhof, and J. Madrenas. 2006. A molecular perspective of CTLA-4 function. *Annu. Rev. Immunol.* 24: 65–97.
14. Sakuishi, K., L. Apetoh, J. M. Sullivan, B. R. Blazar, V. K. Kuchroo, and A. C. Anderson. 2010. Targeting Tim-3 and PD-1 pathways to reverse T cell exhaustion and restore anti-tumor immunity. [Published erratum appears in 2011 *J. Exp. Med*. 208: 1331.] *J. Exp. Med.* 207: 2187–2194.
15. Cavani, A. 2008. T regulatory cells in contact hypersensitivity. *Curr. Opin. Allergy Clin. Immunol.* 8: 294–298.
16. Takahashi, R., Y. Kano, Y. Yamazaki, M. Kimishima, Y. Mizukawa, and T. Shiohara. 2009. Defective regulatory T cells in patients with severe drug eruptions: timing of the dysfunction is associated with the pathological phenotype and outcome. *J. Immunol.* 182: 8071–8079.
17. Azukizawa, H., S. Sano, H. Kosaka, Y. Sumikawa, and S. Itami. 2005. Prevention of toxic epidermal necrolysis by regulatory T cells. *Eur. J. Immunol.* 35: 1722–1730.
18. Grattan, M., Q.-S. Mi, C. Meagher, and T. L. Delovitch. 2002. Congenic mapping of the diabetogenic locus Idd4 to a 5.2-cM region of chromosome 11 in NOD mice: identification of two potential candidate subloci. *Diabetes* 51: 215–223.
19. Koguchi, K., D. E. Anderson, L. Yang, K. C. O'Connor, V. K. Kuchroo, and D. A. Hafler. 2006. Dysregulated T cell expression of TIM3 in multiple sclerosis. *J. Exp. Med.* 203: 1413–1418.
20. Nishimura, H., M. Nose, H. Hiai, N. Minato, and T. Honjo. 1999. Development of lupus-like autoimmune diseases by disruption of the PD-1 gene encoding an ITIM motif-carrying immunoreceptor. *Immunity* 11: 141–151.
21. Niwa, H., T. Satoh, Y. Matsushima, K. Hosoya, K. Saeki, T. Niki, M. Hirashima, and H. Yokozeki. 2009. Stable form of galectin-9, a Tim-3 ligand, inhibits contact hypersensitivity and psoriatic reactions: a potent therapeutic tool for Th1- and/or Th17-mediated skin inflammation. *Clin. Immunol.* 132: 184–194.
22. Faulkner, L., K. Martinsson, A. Santoyo-Castelazo, K. Cederbrant, I. Schuppe-Koistinen, H. Powell, J. Tugwood, D. J. Naisbitt, and B. K. Park. 2012. The development of in vitro culture methods to characterize primary T-cell responses to drugs. *Toxicol. Sci.* 127: 150–158.
23. Mauri-Hellweg, D., F. Bettens, D. Mauri, C. Brander, T. Hunziker, and W. J. Pichler. 1995. Activation of drug-specific CD4+ and CD8+ T cells in individuals allergic to sulfonamides, phenytoin, and carbamazepine. *J. Immunol.* 155: 462–472.
24. Schnyder, B., C. Burkhart, K. Schnyder-Frutig, S. von Greyerz, D. J. Naisbitt, M. Pirmohamed, B. K. Park, and W. J. Pichler. 2000. Recognition of sulfamethoxazole and its reactive metabolites by drug-specific CD4+ T cells from allergic individuals. *J. Immunol.* 164: 6647–6654.
25. Naisbitt, D. J., M. Britschgi, G. Wong, J. Farrell, J. P. H. Depta, D. W. Chadwick, W. J. Pichler, M. Pirmohamed, and B. K. Park. 2003. Hypersensitivity reactions to carbamazepine: characterization of the specificity, phenotype, and cytokine profile of drug-specific T cell clones. *Mol. Pharmacol.* 63: 732–741.
26. Pannetier, C., J. Levraud, A. Lim, J. Even, and P. Kourilsky. 1997. The immunoscope approach for the analysis of T cell repertoires. In *The Antigen T Cell Receptor: Selected Protocols and Applications.* J. R. Oksenberg,ed. R.G. Landes Company, Georgetown, TX, p. 287–325.
27. Hashizume, H., M. Takigawa, and Y. Tokura. 2002. Characterization of drug-specific T cells in phenobarbital-induced eruption. *J. Immunol.* 168: 5359–5368.
28. Daly, A. K., P. T. Donaldson, P. Bhatnagar, Y. Shen, I. Pe'er, A. Floratos, M. J. Daly, D. B. Goldstein, S. John, M. R. Nelson, et al; DILIGEN Study; International SAE Consortium. 2009. HLA-B*5701 genotype is a major determinant of drug-induced liver injury due to flucloxacillin. *Nat. Genet.* 41: 816–819.
29. Chae, S.-C., Y.-R. Park, S.-C. Shim, K.-S. Yoon, and H.-T. Chung. 2004. The polymorphisms of Th1 cell surface gene Tim-3 are associated in a Korean population with rheumatoid arthritis. *Immunol. Lett.* 95: 91–95.
30. Kroner, A., M. Mehling, B. Hemmer, P. Rieckmann, K. V. Toyka, M. Mäurer, and H. Wiendl. 2005. A PD-1 polymorphism is associated with disease progression in multiple sclerosis. *Ann. Neurol.* 58: 50–57.
31. Chuang, W. Y., P. Ströbel, R. Gold, W. Nix, B. Schalke, R. Kiefer, A. Opitz, E. Klinker, H. K. Müller-Hermelink, and A. Marx. 2005. A CTLA4high genotype is associated with myasthenia gravis in thymoma patients. *Ann. Neurol.* 58: 644–648.
32. Donner, H., J. Braun, C. Seidl, H. Rau, R. Finke, M. Ventz, P. G. Walfish, K. H. Usadel, and K. Badenhoop. 1997. Codon 17 polymorphism of the cytotoxic T lymphocyte antigen 4 gene in Hashimoto's thyroiditis and Addison's disease. *J. Clin. Endocrinol. Metab.* 82: 4130–4132.
33. Donner, H., H. Rau, P. G. Walfish, J. Braun, T. Siegmund, R. Finke, J. Herwig, K. H. Usadel, and K. Badenhoop. 1997. CTLA4 alanine-17 confers genetic susceptibility to Graves' disease and to type 1 diabetes mellitus. *J. Clin. Endocrinol. Metab.* 82: 143–146.
34. Gonzalez-Escribano, M. F., R. Rodriguez, A. Valenzuela, A. Garcia, J. R. Garcia-Lozano, and A. Nuñez-Roldan. 1999. CTLA4 polymorphisms in Spanish patients with rheumatoid arthritis. *Tissue Antigens* 53: 296–300.
35. Kouki, T., Y. Sawai, C. A. Gardine, M.-E. Fisfalen, M.-L. Alegre, and L. J. DeGroot. 2000. CTLA-4 gene polymorphism at position 49 in exon 1 reduces the inhibitory function of CTLA-4 and contributes to the pathogenesis of Graves' disease. *J. Immunol.* 165: 6606–6611.
36. Hodi, F. S., S. J. O'Day, D. F. McDermott, R. W. Weber, J. A. Sosman, J. B. Haanen, R. Gonzalez, C. Robert, D. Schadendorf, J. C. Hassel, et al. 2010. Improved survival with ipilimumab in patients with metastatic melanoma. *N. Engl. J. Med.* 363: 711–723.
37. Yang, J. C., M. Hughes, U. Kammula, R. Royal, R. M. Sherry, S. L. Topalian, K. B. Suri, C. Levy, T. Allen, S. Mavroukakis, et al. 2007. Ipilimumab (anti-CTLA4

antibody) causes regression of metastatic renal cell cancer associated with enteritis and hypophysitis. *J. Immunother.* 30: 825–830.
38. Alfirevic, A., F. J. Vilar, M. Alsbou, A. Jawaid, W. Thomson, W. E. R. Ollier, C. E. Bowman, O. Delrieu, B. K. Park, and M. Pirmohamed. 2009. TNF, LTA, HSPA1L and HLA-DR gene polymorphisms in HIV-positive patients with hypersensitivity to cotrimoxazole. *Pharmacogenomics* 10: 531–540.
39. Okajima, M., T. Wada, M. Nishida, T. Yokoyama, Y. Nakayama, Y. Hashida, F. Shibata, Y. Tone, A. Ishizaki, M. Shimizu, et al. 2009. Analysis of T cell receptor Vbeta diversity in peripheral CD4 and CD8 T lymphocytes in patients with autoimmune thyroid diseases. *Clin. Exp. Immunol.* 155: 166–172.
40. Hsieh, Y. C., S. T. Chang, W. T. Huang, S. Y. Kuo, T. A. Chiang, and S. S. Chuang. 2013. A comparative study of flow cytometric T cell receptor Vβ repertoire and T cell receptor gene rearrangement in the diagnosis of large granular lymphocytic lymphoproliferation. *Int. J. Lab. Hematol.* 35: 501–509.
41. Tzifi, F., M. Kanariou, M. Tzanoudaki, C. Mihas, E. Paschali, G. Chrousos, and C. Kanaka-Gantenbein. 2013. Flow cytometric analysis of the CD4+ TCR Vβ repertoire in the peripheral blood of children with type 1 diabetes mellitus, systemic lupus erythematosus and age-matched healthy controls. *BMC Immunol.* 14: 33.
42. Ortonne, N., D. Huet, C. Gaudez, A. Marie-Cardine, V. Schiavon, M. Bagot, P. Musette, and A. Bensussan. 2006. Significance of circulating T-cell clones in Sezary syndrome. *Blood* 107: 4030–4038.
43. Farrell, J., D. J. Naisbitt, N. S. Drummond, J. P. Depta, F. J. Vilar, M. Pirmohamed, and B. K. Park. 2003. Characterization of sulfamethoxazole and sulfamethoxazole metabolite-specific T-cell responses in animals and humans. *J. Pharmacol. Exp. Ther.* 306: 229–237.
44. Callan, H. E., R. E. Jenkins, J. L. Maggs, S. N. Lavergne, S. E. Clarke, D. J. Naisbitt, and B. K. Park. 2009. Multiple adduction reactions of nitroso sulfamethoxazole with cysteinyl residues of peptides and proteins: implications for hapten formation. *Chem. Res. Toxicol.* 22: 937–948.
45. Castrejon, J. L., N. Berry, S. El-Ghaiesh, B. Gerber, W. J. Pichler, B. K. Park, and D. J. Naisbitt. 2010. Stimulation of human T cells with sulfonamides and sulfonamide metabolites. *J. Allergy Clin. Immunol.* 125: 411–418.e4.
46. Gibson, A., M. Ogese, A. Sullivan, E. Wang, K. Saide, P. Whitaker, D. Peckham, L. Faulkner, B. K. Park, and D. J. Naisbitt. 2014. Negative regulation by PD-L1 during drug-specific priming of IL-22-secreting T cells and the influence of PD-1 on effector T cell function. *J. Immunol.* 192: 2611–2621.
47. Parry, R. V., J. M. Chemnitz, K. A. Frauwirth, A. R. Lanfranco, I. Braunstein, S. V. Kobayashi, P. S. Linsley, C. B. Thompson, and J. L. Riley. 2005. CTLA-4 and PD-1 receptors inhibit T-cell activation by distinct mechanisms. *Mol. Cell. Biol.* 25: 9543–9553.
48. Zhu, C., A. C. Anderson, A. Schubart, H. Xiong, J. Imitola, S. J. Khoury, X. X. Zheng, T. B. Strom, and V. K. Kuchroo. 2005. The Tim-3 ligand galectin-9 negatively regulates T helper type 1 immunity. *Nat. Immunol.* 6: 1245–1252.
49. Agata, Y., A. Kawasaki, H. Nishimura, Y. Ishida, T. Tsubata, H. Yagita, and T. Honjo. 1996. Expression of the PD-1 antigen on the surface of stimulated mouse T and B lymphocytes. *Int. Immunol.* 8: 765–772.
50. Takahashi, T., T. Tagami, S. Yamazaki, T. Uede, J. Shimizu, N. Sakaguchi, T. W. Mak, and S. Sakaguchi. 2000. Immunologic self-tolerance maintained by CD25(+)CD4(+) regulatory T cells constitutively expressing cytotoxic T lymphocyte-associated antigen 4. *J. Exp. Med.* 192: 303–310.
51. Hastings, W. D., D. E. Anderson, N. Kassam, K. Koguchi, E. A. Greenfield, S. C. Kent, X. X. Zheng, T. B. Strom, D. A. Hafler, and V. K. Kuchroo. 2009. TIM-3 is expressed on activated human CD4+ T cells and regulates Th1 and Th17 cytokines. *Eur. J. Immunol.* 39: 2492–2501.
52. Walunas, T. L., D. J. Lenschow, C. Y. Bakker, P. S. Linsley, G. J. Freeman, J. M. Green, C. B. Thompson, and J. A. Bluestone. 1994. CTLA-4 can function as a negative regulator of T cell activation. *Immunity* 1: 405–413.
53. Imaizumi, T., M. Kumagai, N. Sasaki, H. Kurotaki, F. Mori, M. Seki, N. Nishi, K. Fujimoto, K. Tanji, T. Shibata, et al. 2002. Interferon-gamma stimulates the expression of galectin-9 in cultured human endothelial cells. *J. Leukoc. Biol.* 72: 486–491.
54. Wherry, E. J., and R. Ahmed. 2004. Memory CD8 T-cell differentiation during viral infection. *J. Virol.* 78: 5535–5545.
55. Golden-Mason, L., B. E. Palmer, N. Kassam, L. Townshend-Bulson, S. Livingston, B. J. McMahon, N. Castelblanco, V. Kuchroo, D. R. Gretch, and H. R. Rosen. 2009. Negative immune regulator Tim-3 is overexpressed on T cells in hepatitis C virus infection and its blockade rescues dysfunctional CD4 + and CD8+ T cells. *J. Virol.* 83: 9122–9130.
56. Jones, R. B., L. C. Ndhlovu, J. D. Barbour, P. M. Sheth, A. R. Jha, B. R. Long, J. C. Wong, M. Satkunarajah, M. Schweneker, J. M. Chapman, et al. 2008. Tim-3 expression defines a novel population of dysfunctional T cells with highly elevated frequencies in progressive HIV-1 infection. *J. Exp. Med.* 205: 2763–2779.
57. Blackburn, S. D., H. Shin, W. N. Haining, T. Zou, C. J. Workman, A. Polley, M. R. Betts, G. J. Freeman, D. A. A. Vignali, and E. J. Wherry. 2009. Coregulation of CD8+ T cell exhaustion by multiple inhibitory receptors during chronic viral infection. *Nat. Immunol.* 10: 29–37.